Available online at www.sciencedirect.com

ScienceDirect

Procedia CIRP 31 (2015) 340 – 345

www.elsevier.com/locate/procedia

15th CIRP Conference on Modelling of Machining Operations

Prediction of temperature induced shape deviations in dry milling

Denkena, B.[a], Schmidt, A.[b], Maaß, P.[b], Niederwestberg, D.[a,*], Niebuhr, C.[b], Vehmeyer, J.[b]

[a]*Institute of Production Engineering and Machine Tools, Leibniz Universität Hannover, 30823 Garbsen, Germany*
[b]*Center for Industrial Mathematics, University of Bremen, 28334 Bremen, Germany*

[*] Corresponding author. Tel.: +49-511-762-4569; fax: +49-511-762-5115. *E-mail address:* niederwestberg@ifw.uni-hannover.de

Abstract

In this paper a model for a simulation based prediction of temperature induced shape deviations in dry milling is presented. A closed loop between Boolean material removal, process forces, heat flux and thermoelastic deformation is established. Therefore, an efficient dexel based machining simulation is extended by a contact zone analysis to model the local workpiece load. Based on the computed contact zone the cutting forces and heat flux are calculated using a semi-empirical process model. For a detailed consideration of the loads they are discretized and localized on the dexel-represented workpiece surface. A projection of the localized workpiece loads on the boundary of the finite element domain, taking into account the Boolean material removal during the process, allows the calculation of the current temperature and deformation of the workpiece. By transforming these thermomechanical characteristics back to the dexel-model a consideration in the machining simulation is possible. An extended contact zone analysis is developed for the prediction of the localized shape deviations. Finally, the results of the simulation are compared with measured data. The comparison shows that workpiece temperatures, workpiece deformation and shape deviations in different workpiece areas are predicted accurately.

Peer-review under responsibility of the International Scientific Committee of the "15th Conference on Modelling of Machining Operations
Keywords: simulation, dry milling, thermal error, deformation, geometric modelling, material removal, finite element method (FEM)

1. Introduction

Shape deviations caused by thermal and mechanical load of the workpiece are a major challenge in dry machining production. Manufacturing errors based on thermal expansion are caused by thermal and mechanical workpiece load. Conventional simulation approaches have to be extended to consider these effects in the simulation of machining processes.

Several investigations discuss the thermal and mechanical effects in machining operations. Based on machining simulations the prediction of cutting forces is a basic approach in modelling of machining operations. In most investigations the cutting forces are calculated time dependently to analyze the process. The consideration of the workpiece deviation is important in machining of thin walled workpiece. Therefore, in [1] a linked simulation of vector based cutting forces and time-dependent elasticity of the workpiece is introduced.

For the analysis of thermal effects in machining operations the Finite Element Method (FEM) is the common approach. It is used for the calculation of the thermal deviation of the workpiece and the prediction of thermal load of the workpiece on the FEM grid by special descriptions of the process kinematics. Including the Boolean material removal process by deleting simplizes [2–4], the resulting model simulates the thermal deviation during drilling and turning processes. These approaches are similar in the description of the process kinematics. Several investigations exist for the modelling of the process by defined thermal load profiles for more challenging process kinematics like milling of free-form workpieces. Therefore, a mesh of the finished workpiece is constructed. The load is projected on the finished workpiece, so that changes of the workpiece size during the processes are not included [5–7]. A similar approach was shown by [8]. A FEM grid of a thin walled workpiece was loaded by forces and heat flux to predict shape deviations. For more flexibility, in [9] a CSG-based modelling of the workpiece load linked with a voxel model for arbitrary machining operations is introduced.

In this paper, a method for modelling of cutting processes is presented to predict the manufacturing errors based on thermal expansion. A CAD-based tool model is intersected with a dexel model and the contact zone is calculated and analyzed. Based on these analysis the incremental workpiece load is predicted. The workpiece load is separated into thermal load by discrete heat input and mechanical load by stress tensors. These loads are projected on the boundary of a finite element domain to calculate the current temperature and deformation of the workpiece. Based on these information the shape deviations generated by the material cutting process are predicted.

Peer-review under responsibility of the International Scientific Committee of the "15th Conference on Modelling of Machining Operations
doi:10.1016/j.procir.2015.03.072

2. General Approach

Deduced from the state-of-the-art the NC-Simulation has to be extended by several properties to emulate thermomechanical effects. These extensions can be divided analytically into two components, the process model and the workpiece model.

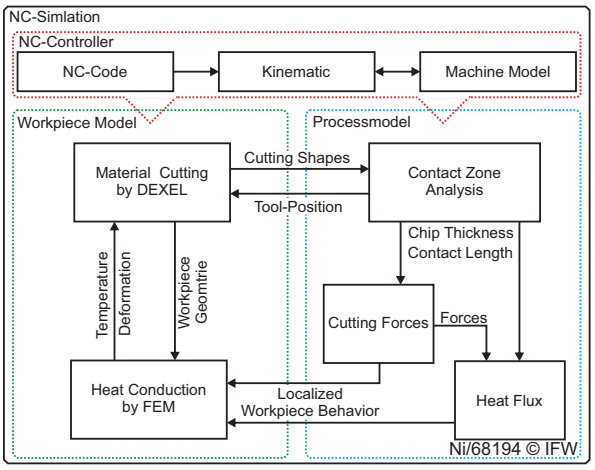

Fig. 1. Detailed Information Flow.

The workpiece model describes the actual state of the workpiece in geometrical and thermomechanical aspects (Fig. 1 left). Additional Boolean removal algorithms allow changing the geometrical representation and the boundary conditions of the workpiece, while thermal conduction algorithms allocate the thermal condition of the workpiece. The process model has several sequences (Fig. 1 right). The cutting conditions are calculated from the intersection of tool and workpiece. With this data a cutting force and heat flux prediction is triggered that calculates the mechanical and thermal load. This changes the boundary conditions of the workpiece model.

The major aspect of this paper is the modelling of shape deviations based on the thermal effects. Linking a dexel model for the machining simulation to a FE model for the heat conduction analysis allows considering both, volumetric changes and thermomechanical deformation, in the NC-Simulation. During the simulation the deformation of the workpiece in the contact zone is analyzed in detail and the local shape deviation of the workpiece is predicted.

2.1. Reference Process

The machining of a thin walled part of 1.1191 steel is chosen as reference process (Fig. 2). The blank part is a rectangular workpiece, which results in a percentage of machined material of about 60%. The part is clamped on two sides, with no degree in freedom of torsion and translation. The sides are fixed on a dynamometer, which enables the measurement of the fixture forces. The machining strategy is z-level constant. The roughing process is divided in two steps for every level. The finishing of the thin wall is performed in one cut.

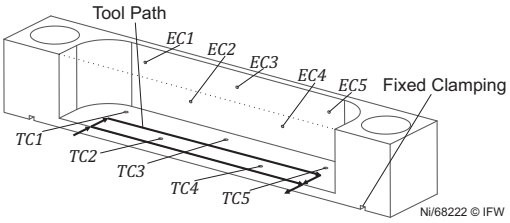

Fig. 2. Reference Process.

3. Modelling

3.1. Geometric Tool Modelling

The common simulation approach of using a body of revolution has to be extended to perform a machining simulation in consideration of the shape of the cutting edge. Therefore, a full three-dimensional model of the detailed tool, which provides the exact tool shape, is required.

The modelling of the tool starts with the discretization of the cutting edge. The edges of the CAD-Model, selected as cutting edge, are sorted in a continuous sequence. Iterating this sequence, every edge is discretized by equidistant linear sections represented by discretization points $P_{ED}(i)$. During the further procedure of the method every section of the discretized edge represents a cutting edge element with individual characteristics. For every discretization point $P_{ED}(i)$, interpolation points $P_{REV,i}(j)$ are created by rotating the discretization point in a user defined angle ω around the tool rotational axis to model the body of revolution. By triangulation of the discretization and interpolation points of two following sections a consistent surface is generated. For further analysis of the contact zone every triangle is allocated to a cutting edge segment. The consistent body of revolution is modelled repeating this triangulation for all cutting edge segments.

Based on data, determined by the tool preparation, the tool reference plane $P_r(i)$ for the i-th cutting edge segment is calculated. The rotation of the tool reference plane $P_r(i)$ from the basic reference plane $P_r(i)$ of the Tool Coordinate System (TCS) is identical with the rotation of the force application point $P_{ED}(i)$ and is called lag angle $\psi(i)$. The lag angle can also be used to characterize the tool geometry and is calculated in relation to a defined start angle point P_{ref} in the coordinate plane. The tool cutting edge angle $\kappa_r(i)$ is the cutting edges orthogonal angular deviation in the reference plane $P_r(i)$, which can be obtained by the vectors connecting the cutting edge discretization points $P_{ED}(i)$. The individually calculated angles (κ_r, ψ) enable the consideration of the local cutting edge of the tool in processing of the local cutting conditions. For the calculation of the resulting cutting forces, individual cutting force coordinate systems for every cutting edge segment are implemented. The cutting force $F_c(i)$ is in the direction of the cutting speed v_c, which is equal to the normal of the tool reference plane n_P. The normal cutting force $F_{cN}(i)$ is equal to the normal of the surface of the modelled tool n_P. The passive force $F_p(i)$ can be modelled orthogonal to $F_c(i)$ and $F_{cN}(i)$.

3.2. Contact Analysis

Each functional part of the tool surface is investigated separately to perform an analysis of the contact zone. Each face is cut with the multidexel model and at each intersection point of a dexel, called Dexel Cut Point (*DCP*), the triangulated surface is assigned to the corresponding cutting edge element. For the *i*-th cutting edge element all *DCPs* are analyzed. The first step in the contact analysis is to calculate the feed direction of the tool. By iterating the movement of all axes the movement of the Tool Center Point (*TCP*) can be calculated in a global coordinate system. The feed direction of the tool corresponds to the difference of the *TCP* from the last to the current simulation step. In the next step, the feed direction of the tool is projected on a plane parallel to the X-Y plane of the tool and defined by the *DCP*. The angular deviation of the *DCP* from the projected feed direction characterizes the contact condition of the *DCP*. By the following relation, the corresponding position angle can be calculated:

$$\varphi_{DCP} = \sphericalangle(v_{f,i}, DCP). \tag{1}$$

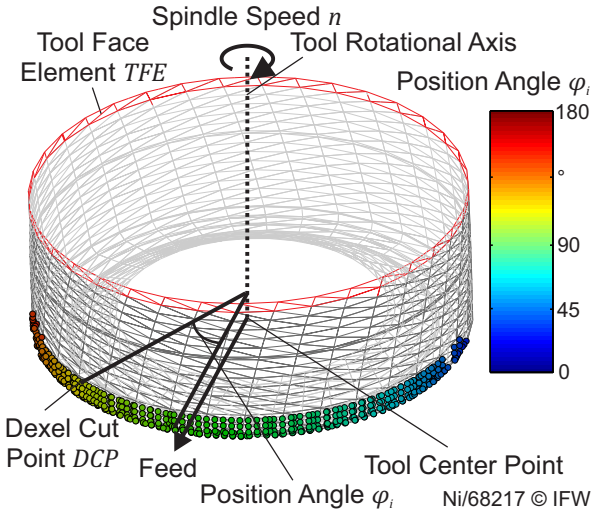

Fig. 3. Contact Analysis of *DCPs* on the Tool of Revolution.

For further analysis the *DCPs* allocated to a tool face element are sorted from entry φ_e to exit φ_a angle by a quicksort algorithm. The workpiece load has to be modelled to simulate and compensate workpiece related thermal and thermomechanical effects. Using the calculated feed the ideal undeformed chip thickness $h_{ideal,DCP}$ can be calculated for every DCP:

$$h_{ideal,DCP} = f_z \cdot sin(\varphi_{DCP}). \tag{2}$$

For processing of the undeformed chip thickness h_{DCP} the cutting edge individual characteristics i.e. cutting edge angle of the tool are considered. Further, the ramping angle α_i, which is the deviation of the feed direction from spindle axis orientation (SAO) of the tool, has to be calculated. The ramping angle is calculated by the following equation:

$$\alpha_i = \sphericalangle(v_{f,i}, SAO) - 90°. \tag{3}$$

Furthermore, the undeformed chip thickness is by calculated by

$$h_{DCP} = h_{ideal,DCP} \cdot cos(\kappa_i - \alpha_i). \tag{4}$$

The contact analysis is done for the whole process. In every simulation step the dexel based workpiece representation is intersected by the modelled tool. For the discretization of the workpiece (48 x 48 x 195 mm^3) 64 x 64 x 256 Dexel are chosen. Figure 4 shows the contact zone of a single simulation step. The detected DCPs are allocated to the position on the cutting edge and the position angle. Responding to the movement of the tool the corresponding undeformed chip thickness is calculated for each *DCP*. The entry and exit angle for the simulation step is described as a polygon, connecting the minimum and maximum position angle.

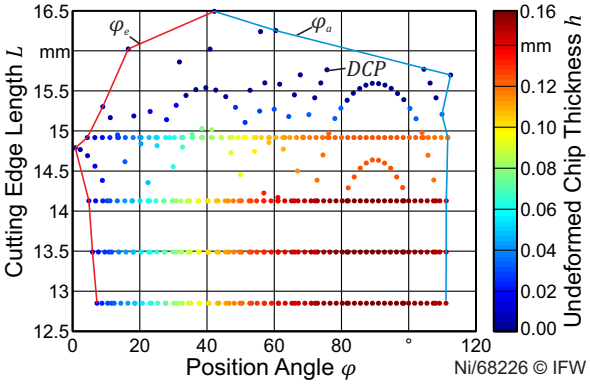

Fig. 4. Contact Analysis of a Single Simulation Step.

3.3. Process Modelling

The process model is a data-driven estimation of process forces and heat flux and provides the loads for the heat equation. The function-based model is an obvious modelling approach and accurately within a certain range of process parameters. The input variables are determined within the simulation environment, which makes it possible to use instantaneous and local chip thickness $h = h(t, s)$. As depicted in the data flow diagram in Fig. 1, heat flux is modeled in two stages. The first step is the determination of process forces. Force modelling is a well known discipline but the main attraction is the possibility of direct measurement and validation. Under the assumption that mechanical work is totally converted into heat, the second part of the process model is an empirical quantifier of the proportion of the total heat that is flowing into the workpiece. Both stages are described in the following.

3.3.1. Force Modelling

The Forces are estimated by

$$F = \mathcal{A}k, \tag{5}$$

where k represents the specific force and $\mathcal{A}$ the linear force operator. The operator $\mathcal{A}$ depends on the force model, the static tool shape and the dynamic simulation variables kinematics and tool engagement. If the specific force k is known, (5) is a prediction of forces. Applying $\mathcal{A}$ in an inverse way, leads to an identification method of specific forces from measured data. This regression is done in the sense of least squares by solv-

ing the minimization problem

$$\|\mathcal{A}k - F_{meas}\|_2^2 \rightarrow \min_k . \tag{6}$$

The whole force model with identification of specific forces for different engagement conditions as well as a validation of the force prediction for different cutting conditions is shown in detail in [14]. In the following, the main steps are briefly presented.

The specific forces are modeled as a polynomial of uncut chip thickness. Polynomials are chosen because of the ability to approximate a nonlinear behavior and their computational advantages. Let the polynomial of uncut chip thickness and of degree $p-1$,

$$K = K(h) = \sum_{i=0}^{p-1} k_{i+1} h^i, \quad p > 0 \tag{7}$$

be the specific cutting force. With familiar approach the cutting force results by multiplication of the cross section of undeformed chip $A_c \approx bh$ and in addition an additive constant friction term. Accordingly, it follows

$$F_c = Kbh + k_0 b = bh \sum_{i=0}^{p-1} k_{i+1} h^i + k_0 b = b \sum_{i=0}^{p} k_i h^i. \tag{8}$$

For $p := 1$ there is $F_c = [k_1 h + k_0]b$, which is the well known two component shear-friction model. For higher degrees a nonlinear shear force is estimated. The approach (8) is set up for the three force directions, furthermore the forces are transformed into the stationary measurement coordinate system and integrated along each cutting edge:

$$F(t,s) = \int_0^L R(t,s) \sum_{i=0}^{p} \begin{pmatrix} k_{i,cN} \\ k_{i,c} \\ k_{i,p} \end{pmatrix} h(t,s)^i ds. \tag{9}$$

In further steps the integral in (9) is discretized, the coefficients are factored out and the linear force operator $\mathcal{A}$ is assembled. An in-process identification of specific forces is possible through efficient solving of (6) and automatic time synchronization with measurement, the interested reader is refered to [14].

The mechanical load on an individual part of the contact zone is given for all DCPs by the normed vector:

$$F_{DCP} = \frac{F(t_{DCP}, s_{DCP})}{A_{DCP}}. \tag{10}$$

The area of action for a *DCP* is limited by the operation area of the cutting edge segment b_i and the distance to the following *DCP* of the segment:

$$A_{DCP} = b_i \cdot (\varphi_{DCP-1} - \varphi_{DCP}) \cdot d_{DCP}. \tag{11}$$

3.3.2. Empirical Approach For The Induced Heat

Starting point for the heat flux model is the validated force model (5). No direct measurement of heat flux is possible, therefore an indirect calibration campaign has been developed. Its main aspects are described in the following. The quantifier $w(h, v_c) \in [0\%, 100\%]$ gives the proportion of the total heat (mechanical work) flowing into the workpiece. The function-based approach needs initial measurement for the primary influencing factors, which have been identified as the cutting velocity v_c and the uncut chip thickness h. To simulate the behavior for different uncut chip thicknesses, slot milling with overlappings between 25% and 100% have been performed, so that different mean chip thicknesses $\bar{h}$ arise. With the cutting force

$$F_c = \sum_{i=0}^{p} k_i h^i, \quad p > 0, \tag{12}$$

the resulting power is

$$P_c = F_c v_c = \left(\sum_i k_i h^i \right) v_c. \tag{13}$$

The total work produced by a single turn is

$$W_{\text{total}} = \int_0^{2\pi} P_c \, d\phi = \int_0^{2\pi} \left(\sum_i k_i h^i \right) v_c \, d\phi = 2\pi \sum_i k_i \bar{h}^i. \tag{14}$$

With the prior assumption, W_{total} is completely converted into heat. The energy Q of the workpiece is determined indirectly with help of homogenization temperatures and as a result the (mean) heat flux is determined by

$$\dot{Q} = \frac{Q}{\Delta t_{\text{mill}}}, \tag{15}$$

where Δt_{mill} denotes the duration of heat induction. Equating the work performed by a single turn with (15),

$$\frac{Q}{\Delta t_{\text{mill}}} = w \cdot \frac{W_{\text{total}}}{\Delta t_{\text{turn}}} \tag{16}$$

leads to the quantifier w. The final quantifier $w = w(h, v_c)$ is a regression function of 61 experiments with different cutting velocities and mean chip thicknesses $\bar{h}$. Moreover, the quantifier is used to calculate the local induced heat flux for each DCP:

$$\dot{Q}_{DCP} = w(h_{DCP}, v_{c,DCP}) \cdot F_{DCP} \cdot v_{c,DCP}. \tag{17}$$

Further, the thermal workpiece load is modelled as heat input. Therefore, local dissipated heat flux has to be converted into the heat with respect to the time of action:

$$Q_{DCP} = \dot{Q}_{DCP} \cdot \Delta t, \quad \text{with } \Delta t = (\varphi_{DCP-1} - \varphi_{DCP}) \cdot \frac{1}{n}. \tag{18}$$

Overall, this method allows the local discretized simulation of the thermal and mechanical workpiece load.

3.4. Thermomechanical Modelling

The model of thermomechanical effects during machining processes includes the classical formulations of the heat equation and the quasi-stationary elasticity equation on time dependent domains with moving boundary conditions. The coupled system is discretized and simulated with the adapted finite element toolbox ALBERTA, [10]. This toolbox uses unstructured simplicial meshes together with local adaptive mesh refinement and coarsening for appropriate approximations of domain and solution.

This machining simulation and thus time dependent domain is realized by using a time dependent subset of a fixed domain $\Omega = \Omega_s(t) \cup \Omega_m(t) \cup \Gamma(t) \subset \mathbb{R}^3$. Thereby, Ω is divided into a solid subdomain $\Omega_s(t)$ and a removed subdomain $\Omega_m(t)$. The subdomain boundary $\partial\Omega_s(t)$ is subdivided in parts with different boundary conditions, like Neumann $\Gamma_N(t)$ and/or Robin conditions $\Gamma_R(t)$. The data at the boundaries are given by the process

model, see Section 3.3. Heat fluxes and process forces, have to be given on $\partial\Omega_s(t)$, which is at least partly composed of interior sides of elements of the original triangulation of Ω.

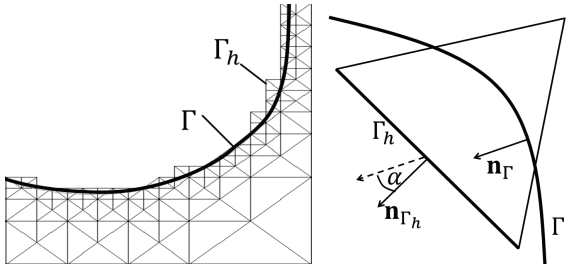

(a) Exact and discrete boundary overlay (b) Normal projection on simplex

Fig. 5. Sketches of boundary projection in FEM.

During the approximation of the current workpiece surface by the FEM, we typically get for the discretized boundary $\partial\Omega_{s,h}(t)$ a larger surface area, than for the relatively smooth surface given by the geometrical information from the dexel model, see Figure 5(a). An adaption to the boundary is necessary. The difference between the integrals over the discrete and continuous boundaries can be corrected by the scalar product of the cosine of the enclosed angle α between the two normal vectors (Fig. 5(b)).

The linking of the dexel model and the FEM is based on the interchange of parameters and values such as surface of the workpiece geometry as well as heat flux and process forces produced by the cutting process. A detailed description of the linking is given in [11], [12].

Through the different discretizations in FEM and dexel model in space and time, only information from a few DCPs could be assigned to the boundary of a simplex. Bilinear interpolation over each dexel field is used to compensate this. For each quadrature point x, 4 supporting points $\tilde{q}_i^k$ exists over each dexel field k. thus, there is heat flux data

$$\tilde{q}_i^k = Q_{DCP}^k \cdot \cos\alpha(\mathbf{n}_{\Gamma_{N,h}}, \mathbf{n}_{DCP}^k) \tag{19}$$

with thermal load Q_{DCP}^k from (18) and normal vector $\mathbf{n}_{DCP}^k$ of the continuous surface $\Gamma(t)$. With interpolation operator I_h, there holds finally for the discrete Neumann boundary condition

$$\int_{\Gamma_{N,h}(t)} -\kappa_h \nabla\Theta(x,t) \cdot \mathbf{n}\, \psi(x)\, \mathrm{d}x = \int_{\Gamma_{N,h}(t)} q_h(x,t)\psi(x)\, \mathrm{d}x \tag{20}$$

with FE test functions ψ and $q_h(x,t)$ at quadrature point x,

$$q_h(x,t) = \frac{1}{\Delta t} \sum_{k=1}^{d} I_h(x, \tilde{q}_1^k, \tilde{q}_2^k, \tilde{q}_3^k, \tilde{q}_4^k) \tag{21}$$

with d the number of given dexel fields and time step Δt as defined in (18). Analogous, there is data for the weak formulation of the Neumann boundary condition of the elasticity equation

$$\int_{\Gamma_{N,h}(t)} -\sigma(\mathbf{U}(x,t)) \cdot \mathbf{n}\, \psi(x)\, \mathrm{d}x = \int_{\Gamma_{N,h}(t)} \mathbf{f}_h(x,t)\psi(x)\, \mathrm{d}x. \tag{22}$$

Thereby is the vector function $\mathbf{f}_h(x,t)$ defined as $q_h(x,t)$ in (21) with mechanical load F_{DCP} from (10) instead of the thermal load Q_{DCP} above.

Using these modifications for the boundary data from the dexel model, this gives a good approximation of thermomechanical deformation and workpiece temperature in the FEM, see section 4.

3.5. Shape Deviation Prediction

The geometric representation of the workpiece by a dexel model is extended by thermomechanical information to consider the thermomechanical effects in the machining simulation. Temperature and deformation of the workpiece are specific data and have to be known when analyzing the information demand. The data structure of the dexel model enables a geometric representation of the workpiece surface by discrete start and endpoints of the dexel elements. In cutting operations only near-surface areas are machined. Caused by this fact only information in these areas of the workpiece is relevant for a machining simulation. Therefore, an extension of the existing structure is only necessary in the start and endpoints of the dexel. To consider temperature and deformation a dexel point was extended by a temperature value and a deformation vector.

Current thermomechanical data, continuously imported from the thermomechanical model in the dexel structure, now allows considering the thermomechanical effects in the NC-Simulation. These effects are caused by the local temperature and the local deformation of the workpiece in the cutting zone.

The deformation of the workpiece influences the dimension of the contact zone and the geometric representation of the workpiece. Therefore, the deformation determined by analyzing the *DCPs* is projected negative on the tool model. By this method the thermomechanical deformation of the workpiece can be considered and the resulting shape deviation can be predicted. Furthermore, for every cut dexel the current negative vector of deformation is stored in the dexel field for a detailed analysis of the resulting shape.

4. Results

As a first result the estimated temperatures of simulation and measurement are compared at the positions of the thermocouples (TE) in the workpiece bottom area (Fig. 6). There is a significant correlation between the measured and simulated temperatures in magnitude and characteristic. While the part is machined in roughing mode the temperature rises in the workpiece until a peak is reached. During the finishing process of the part the temperature, measured at the bottom area of the workpiece, falls until a second peak is reached when the bottom of the workpiece is machined.

The deformation of the workpiece at the measured position of the eddy current (EC) sensors rises during the roughing of the workpiece, while it is on a constant level during finishing of the part. Peaks in the plot show the passing of the heat source that results in an additional deformation of the workpiece (Fig. 7). The difference of measured and simulated deformation, especially during finishing, can be explained by unknown clamping forces which cannot be modelled.

The resulting error of the shape shows the influence of local different deformations of the workpiece when the final shape of the workpiece is cut (Fig. 8). For every z-level of the workpiece the maximum error decreases.

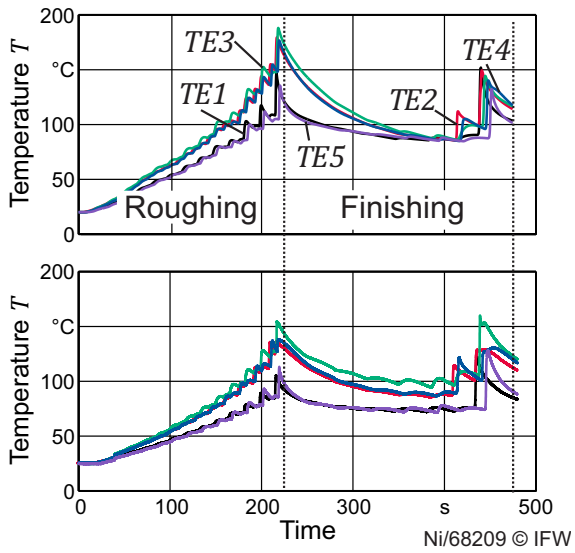

Fig. 6. Temperature in the Workpiece. Top: Simulated, Bottom: Measured.

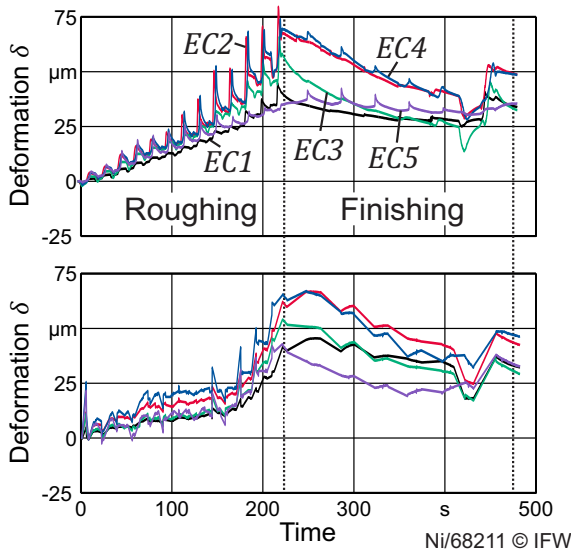

Fig. 7. Deformation of the Workpiece. Top: Simulated, Bottom: Measured.

5. Conclusion and Outlook

In the present paper a method for NC-Simulation based prediction of temperature induced shape deviations is presented. In the first part of the paper the modelling of the rotational tool from a CAD-Model was shown. Tool and dexel represented workpiece are intersected to perform a contact-analysis. The intersection points on the tool are analyzed including technological information stored in the discretized tool. To model the workpiece load for every intersection point, the thermal and mechanical load was calculated using cutting force and heat partition models. The comparison of measured and simulated temperatures and deformations of a real process proved the performance of the method. The influence of varying cutting conditions on the resulting error is reproduced well.

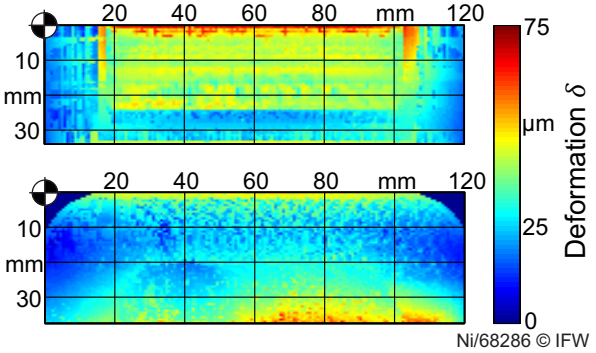

Fig. 8. Predicted Shape Deviation. Top: Thin Workpiece Wall, Bottom: Thin Workpiece Bottom.

Acknowledgments

The presented results have been obtained within the research project "Thermomechanical Deformation of Complex Workpieces in Drilling and Milling Processes" (DE 447/90-2, MA 1657/21-2) within the DFG Priority Program 1480 "Modeling, Simulation and Compensation of Thermal Effects for Complex Machining Processes". The authors would like to thank the DFG for its financial and organizational support of the project.

References

[1] Kersting, P., Biermann, D., Modeling Techniques for the Prediction of Workpiece Deflections in NC Milling, Procedia CIRP, 2, 2012, 83-86.
[2] Bono, M., Jun Ni, The effects of thermal distortions on the diameter and cylindricity of dry drilled holes, International Journal of Machine Tools and Manufacture, 41/15, 2001, 2261-2270.
[3] Isbilir, O., Elaheh G., Finite element analysis of drilling of titanium alloy, Procedia Engineering, 10, 2011, 1877-1882.
[4] Zimmermann, M., et al. Analysis of Thermo-Mechanical effects on the machining accuracy when turning aluminium alloys, 2012.
[5] Fleischer, J., R. Pabst, and S. Kelemen, Heat flow simulation for dry machining of power train castings, CIRP Annals-Manufacturing Technology, 56/1, 2007, 117-122.
[6] Neugebauer, R., et al. Thermal Interactions between the Process and Workpiece, Procedia CIRP, 4, 2012, 63-66.
[7] Schmidt, C., Einflussgrössensensitive Simulation und Überwachung von Fräsprozessen., Berichte aus dem IFW, 2011, PZH Produktionstechnisches Zentrum.
[8] Denkena, B., Schmidt, C, Krüger, M., Experimental investigation and modeling of thermal and mechanical influences on shape deviations in machining structural parts, International Journal of Machine Tools and Manufacture, 50/11, 2010, 1015-1021.
[9] Surmann, T., et al. Simulation of the Temperature Distribution in NC-Milled Workpieces, Advanced Materials Research, 223, 2011, 222-230.
[10] Schmidt A., Siebert K.G., Design of Adaptive Fnite Element Software: Finite Element Toolbox ALBERTA, Springer Heidelberg, 2005.
[11] Niebuhr C. Niederwestberg D., Schmidt A., Finite Element Simulation of Macroscopic Machining Processes - Implementation of time dependent Domain and Boundary Conditions, University of Bremen, 2014; 14-01.
[12] Denkena B., Schmidt A., Henjes J., Niederwestberg D., Niebuhr C., Modeling a Thermomechanical NC-Simulation, Procedia CIRP,8:69-74,2013.
[13] Denkena B., Boess V., Bruening J., Concurrent Engineering Approaches for Substainable Product Developement in Multi-Disciplinary Envoriment, Springer London, 2013.
[14] Denkena, B.; Vehmeyer, J.; Niederwestberg, D.; Maaß, P; Identification of the specific cutting force for geometrically defined cutting edges and varying cutting conditions, International Journal of Machine Tools and Manufacture, 2014, 82-83, 42-49. doi:10.1016/j.ijmachtools.2014.03.009.